^{3}H bound state for the Reid soft-core potential: Exact calculation by a perturbational approach

T. Sasakawa
Department of Physics, Tohoku University, 980 Sendai, Japan

T. Sawada
Department of Applied Mathematics, Faculty of Engineering Science, Osaka University, 560 Toyonaka, Japan
(Received 21 August 1978)

The perturbational approach to the Faddeev equation proposed by us is applied to the ^{3}H bound state. The perturbation iteration is found to converge beautifully, leaving no question about its usefulness. Using the Reid soft-core potential, we obtain the ^{3}H binding energy at 6.62 MeV, $P(S) = 90.28\%$, $P(S') = 1.70\%$, and $P(D) = 8.02\%$, for the three-body state consisting of the two-body pair in the $^1S_0$ and the $^3S_1 + {}^3D_1$ state with the third particle in the s-state relative to the center-of-mass of the pair. The contribution from the third particle in the d-state adds to the binding energy only a small fraction (~ 0.05 MeV). The one-body charge form factor of ^{3}He has a dip at $q^2 \sim 16$ fm^{-2}, and the height of the second peak is about an order of magnitude too low compared to the data. Each Faddeev component of the triton wave function as a function of the relative distance of a pair has a node near the core radius in its $^1S_0$ and $^3S_1$ components, but no node is found in the $^3D_1$ component. The wave function as a function of the spectator coordinate extends over quite large distances without a node in any component. The nodes are attributed to the strong soft-core and the particle exchange effects.

[NUCLEAR STRUCTURE Triton bound state. Exact solution of the Faddeev equation by a perturbative approach. Binding energy; 6.62 MeV. Node of the wave function near the core radius.]

I. INTRODUCTION

It has long been a problem in nuclear physics to know to what extent the effect of three-body forces and the off-shell properties of a two-body potential influence nuclear properties of three- and more-than-three-body systems. Obviously, the triton is the most suited object to study these questions. The first step, of course, is to solve the three-body problem assuming that the interaction Hamiltonian is given by a sum of realistic two-body potentials to see if we get the correct binding energy of the triton, the charge form factor, etc.

After a long history of calculating the wave function and the binding energy of the triton by variational methods,[1,2] people began to calculate these quantities on the basis of the Faddeev integral equation.[3] In general, the variational method is an effort to approach the correct wave function by making the detour of not solving the Schrödinger equation directly. This is in contrast to solving the Schrödinger equation expressed in the form of an integral equation, in which we impose correct boundary conditions and make our effort to obtain an *exact* solution if the integral equation is amenable to numerical calculations.

At an early stage of the studies of a three-body problem, it was felt that solving a Faddeev equation that is a two-dimensional coupled set of integral equations was impossible on existing computers. As a result, various separable approximations of the two-body t matrix were introduced with the purpose of reducing the Faddeev integral equation to a set of coupled integral equations of one variable. However, since a local potential is not a Hilbert-Schmidt operator, the t matrix for a local potential can not exactly be expressed as a sum of separable terms.[4] In this context, we introduce the work "exact" meaning "without recourse to a separable expansion of the t matrix." In view of the importance of solving the three-body system exactly, we report the result of an *exact* calculation of a three-nucleon bound state based on a method quite different from other authors. We use the Reid soft-core (RSC) potential as a typical two-nucleon potential.[5]

So far, the Faddeev equation for the three-nucleon bound state with the RSC potential has been solved exactly by two methods; the Padé approximant[6,7] and the partial differential equations.[8]

In Refs. 6 and 7, the problem was handled in momentum space. In this case we must calculate a great number of matrix elements. This situation seriously restricts the number of mesh points. In Ref. 7, for example, ten and sixteen points are chosen for the spectator and the relative motion in momentum space, respectively. If the number of the coupled integral equation is five as in Ref. 7,

this means that we are handling a 800×2 matrix for each step. We want to avoid this difficulty. Furthermore, we have the problem of reproducing faithfully the detailed feature of the sophisticated RSC potential, which has originally been given in coordinate space. Thus, we choose to calculate the relative motion of a pair of particles in coordinate space. In fact, in our calculations, we use 30 uneven x-mesh points from $x=0$ to 6 fm with the mesh size ranging from $x=0.0270$ fm at $x=0$ to 0.725 fm at $x=6$ fm, and an analytical formula beyond 6 fm. This procedure yields wave functions which are so accurate that further improvement in numerical procedure is unnecessary for calculations of the relative motion. We may say that our calculation of the relative motion is exact. For the spectator, we use the momentum space representation with twelve mesh points.

Details about the formulas have been given in other technical reports.[9-11] Here we write the background and the outline of our method. Our primary concern in the formulation is to have an accurate and practical method of calculation easily accessible to anybody. For that purpose, we must make the size of the matrix as small as possible, so that we can use the computer memory and time for accurate calculations of matrix elements. Further, we must avoid expansion in a complete set of orthonormal functions, whether in the hyperspherical functions,[12] in the Sturm-Liouville functions,[13] in the Kapur-Peierls states,[14] or in the harmonic oscillator functions.[15] These expansions may be correct in principle, but are always troubled by the question of convergence in practice.[2,16] For instance, suppose that for the t matrix at negative energies ($E<0$) we use the Sturm-Liouville functions up to a very large $|E|$. If $|E|$ becomes large, the convergence of matrix elements which appeared in the three-body calculation becomes very slow due to the increase in the normalization factor.[14,17] Furthermore, since the Sturm-Liouville function of order n has $(n-1)$ nodes inside the force range and hence oscillates violently and peaks sharply as n increases, the three-body calculations become less and less accurate with increasing n. This difficulty and the difficulty due to increasing dimensionality of the matrix prevent us from employing the Sturm-Liouville functions up to a large n. In practice, we are forced to truncate the expansion at $n=3$ or less.

Our basic idea in the present paper is a perturbative approach.[17-19] There are two crucial points for any perturbation method. Firstly, the perturbed part must be chosen so that it converges after some successive iterations. Secondly, the unperturbed part must easily be calculated. In the three-body problem, there are many possibilities in choosing the unperturbed part; the Yamaguchi interaction,[20] the first Sturm-Liouville function,[21] the unitary pole approximation,[22] and so forth. Anyway, it is almost evident that the contribution from the poles of the two-body system must be included in the unperturbed part. Then all the rest may be treated as the perturbation. To get an exact result, the perturbational calculations must converge in such a way that no question about the convergence and the accuracy is left. Our preliminary calculation shows that in the region where the Sturm-Liouville expansion becomes impracticable, the perturbation iteration converges rather quickly.

More specifically, we start from the Faddeev equation for the three-body wave function in coordinate space. In the present calculation, the RSC potential acting on the ${}^1S_0$ and the ${}^3S_1+{}^3D_1$ two-body state is used. The spectator particle is then restricted to $l=0$ and 2 relative to the center-of-mass of the pair. We shall report on the results with $l=0$ mostly, but the result of the binding energy including $l=2$ will also be given. First we expand the three-body Faddeev equation by the plane wave states of the spectator particle. To each momentum p of the spectator particle corresponds momentum q of the pair through the relation

$$|q|=(m|E|/\hbar^2+3p^2/4)^{1/2} \quad (q=i|q|),$$

where $|E|$ denotes the trial triton binding energy. Henceforth, we use the notation q in place of $|q|$, for simplicity. For each q, we have the Faddeev equation which we treat in coordinate space. For the momentum q ranging from $(m|E|/\hbar^2)^{1/2}$ to an appropriately chosen value q_M, we calculate the first Sturm-Liouville functions of the ${}^1S_0$ and the ${}^3S_1+{}^3D_1$ two-body states. These functions are used to make the Faddeev equation for these two states in this range of q separable. This part alone constitutes the three-body problem of one variable and is treated as the unperturbed part in the whole problem. The contribution from all the rest, the ${}^1S_0$ and the ${}^3S_1+{}^3D_1$ states in the range beyond q_M, as well as all other two-body states in the the entire range $q>(m|E|/\hbar^2)^{1/2}$, is treated as the perturbation. We take the maximum value of p as 1.95 fm^{-1}, which is shown to be sufficient (see, Fig. 11). As mentioned above, the basis set of functions need not be the first Sturm-Liouville functions. However, this set makes the formulation simpler than any other choice. The formulation is done in the form of integral equations, while numerical calculations are performed by means of equivalent ordinary differential equations with inhomogeneous terms.

By the present method, when the Faddeev equa-

tion is expressed in a matrix form, the dimensionality of the matrix is rather small. It is $mN\times mN$, where m is the number of the two-body state ($m=2$ for $^1S_0$ and $^3S_1+^3D_1$), and N is the number of mesh in momentum for $q\leq q_M$. (In Sec. II and thereafter, the number mN is called the number of the basic states.) We choose $N=6$ for "the standard p mesh," which is defined in Sec. VI. This smallness of the dimensionality of our matrix enables us to perform the calculation of each matrix element to sufficient accuracy. As will be seen, the perturbation converges beautifully within a few steps regardless of the choice of q_M, thus leaving no question about the convergence and the accuracy.

In Sec. II, we summarize our basic formulas. Since the detailed formulation has already been given,[9-11,17-19] we shall present it as brief as possible. In Sec. III, we discuss the details of the calculation. In Sec. IV, we demonstrate, using ^1S and ^3S central potentials, that the perturbation converges regardless of q_M. The results of the calculation for the RSC potential are presented in Sec. V. Discussions and conclusions are given in Sec. VI.

II. DEFINITIONS AND BASIC FORMULAS

We use the set of coordinates and momenta

$$\vec{x}=\vec{r}_1-\vec{r}_2,\quad \vec{y}=\vec{r}_3-(\vec{r}_1+\vec{r}_2)/2 \tag{1}$$

and

$$\vec{q}=\tfrac{1}{2}(\vec{k}_1-\vec{k}_2),\quad \vec{p}=\tfrac{2}{3}[\vec{k}_3-(\vec{k}_1+\vec{k}_2)/2]. \tag{2}$$

we denote by $|a\rangle$ and $|\alpha\rangle$ the normalized spin-isospin-angular function of a two-body and a three-body state, respectively. For a given q and a, where a is the $^1S_0$ or the $^3S_1+^3D_1$ state, we define the first Sturm-Liouville function $\psi_a(q,x)$ by the solution of the equation

$$G^{(2)}_{0,a}(q)V_a\psi_a(q)=\lambda_a(q)\psi_a(q), \tag{3}$$

with the largest eigenvalue λ_a. We normalize the function ψ_a by

$$\langle\psi_a|V_a|\psi_a\rangle=-\lambda_a(q)/[1-\lambda_a(q)]. \tag{4}$$

In Eq. (3), V_a is the two-nucleon potential multiplied by $m/\hbar^2$. The two-body Green's function $G^{(2)}_{0,a}(q)$ is defined by

$$\left(-q^2+\frac{d^2}{dx^2}+\frac{2}{x}\frac{d}{dx}-\frac{L(L+1)}{x^2}\right)G^{(2)}_{0,a}(q;x,x')=\frac{\delta(x-x')}{xx'}. \tag{5}$$

As the boundary condition to this Green's function, we require that it be regular at the origin and decrease exponentially at large distances from the origin. In terms of the function ψ_a, we can express the Green's function as

$$G^{(2)}_{0,a}(q)=-[1-\lambda_a(q)]|\psi_a\rangle\langle\psi_a|+g_a(q). \tag{6}$$

This equation defines the new Green's function $g_a(q)$. Of course, we can write out a more general formula in which any number of Sturm-Liouville functions are involved. However, we use Eq. (6) in the present paper. The reason is explained in Sec. IV. In the usual perturbation methods, the *potential* is divided into an unperturbed part and the remainder which is treated as the perturbation. In our approach, the *Green's function* is divided into an unperturbed part and the remainder which is treated as the perturbation. This division of the Green's function is essential for achieving convergence in successive iterations irrespective of the strength of the potential.[17,23]

Associated with the Green's function $g_a(q)$, we define the wave matrix $\omega_a(q)$ by

$$\omega_a(q)=1+g_a(q)V_a\omega_a(q). \tag{7}$$

Then we can show that[17]

$$G^{(2)}_{0,a}(q)t_a(q)=-|\psi_a(q)\rangle\langle\psi_a(q)|V_a+[\omega_a(q)-1]. \tag{8}$$

This decomposition will be used for the $^3S_1+^3D_1$ and the $^1S_0$ states when q is in the region $(m|E|)^{1/2}/\hbar\leq q\leq q_M$. These will be called the basic states. For the $^3S_1+^3D_1$ and the $^1S_0$ states in the region $q>q_M$, as well as for higher partial waves for all values of q, we will use $G^{(0)}_{0,a}(q)t_a$ as a whole without the decomposition of Eq. (8). In treating the three-body problem, we consider the first term on the right-hand side of Eq. (8) as the unperturbed part, and all the rest as the perturbation.

The totally antisymmetric three-body bound state with $T=M_T=\frac{1}{2}$ is given by[18]

$$\Psi=\Phi(12,3)+\Phi(23,1)+\Phi(31,2), \tag{9}$$

where

$$\Phi(12,3)=\zeta''(12,3)\psi^A(12,3)+\zeta'(12,3)\psi^S(12,3), \tag{10}$$

and similarly for $\Phi(23,1)$ and $\Phi(31,2)$. Here ζ'' and ζ' denote the three-body isospin function $|(I\tfrac{1}{2})TM_T\rangle$; $\zeta''=-|(1,\tfrac{1}{2})\tfrac{1}{2}\tfrac{1}{2}\rangle$ and $\zeta'=|(0,\tfrac{1}{2})\tfrac{1}{2}\tfrac{1}{2}\rangle$. Also,

$$\psi^{S(A)}(12,3)=\sum_{\alpha}^{S(A)}|(LS)J,(l\tfrac{1}{2})j;J_0M_0(12,3)\rangle\phi_\alpha(x,y), \tag{11}$$

where $\sum_\alpha^{S(A)}$ stands for the sum over $\alpha=\{LSJlj(12,3)\}$ with symmetric (antisymmetric) spatial-spin states with respect to the pair 12. $|(LS)J,(l\tfrac{1}{2})j;J_0M_0(12,3)\rangle$ is the normalized spin-angular wave function in which the state $|(LS)J\rangle$

for the pair 12 and the state $|(l\frac{1}{2})j\rangle$ for the spectator are combined to form the total state $|J_0M_0\rangle$ ($J_0=\frac{1}{2}$ for ^3H).

We designate by $G_0^{(3)}$ the Green's function in the three-body free space. First, we expand $G_0^{(3)}t$ in terms of the complete set of the normalized plane wave state of the spectator particle. We denote by $u_l(p,y)$ the normalized spherical Bessel function,

$$|u_l(p)\rangle = u_l(p,y) = \sqrt{2/\pi}\, p j_l(py). \tag{12}$$

We designate by t_a the scattering matrix for the two-body state a. If we use Eqs. (8) and (12), $G_0^{(3)}t_a$ is expressed as

$$G_0^{(3)}t_a = \sum_\alpha{}' \int' dp\,|u_l(p)\rangle|\alpha\rangle\{-|\psi_a(q)\rangle\langle\psi_a(q)|V_a + [\omega_a(q)-1]\}\langle\alpha|\langle u_l(p)|$$
$$+\left(\sum_\alpha{}' \int'' dp + \sum_\alpha{}'' \int_0^\infty dp\right)|u_l(p)\rangle|\alpha\rangle G_{0,a}^{(2)}(q)t_a(q)\langle\alpha|\langle u_l(p)|, \tag{13}$$

Here $\sum'_\alpha$ ($\sum''_\alpha$) is the sum over the basic states (the sum over states other than the basic states), and $\int' dp$ ($\int'' dp$) is the integration over the region of p corresponding to the values of q in the region $(m|E|)^{1/2}/\hbar \leqslant q \leqslant q_M (q > q_M)$. The relation between p and q has been given in Sec. I.

The Faddeev equation for a three-body bound state is given by

$$|\Phi\rangle = G_0^{(3)}tA|\Phi\rangle, \tag{14}$$

where the operator A transforms $\Phi(12,3)$ into $\Phi(23,1)+\Phi(31,2)$. Using Eq. (13) into Eq. (14), thereby treating the term with $-|\psi_a(q)\rangle\langle\psi_a(q)|V_a$ as the unperturbed term and the rest as the perturbation, we find

$$A|\Phi\rangle = -B\sum_{\alpha_1}{}' \int' dp_1 A|u_{l_1}(p_1)\rangle|\alpha_1\rangle \times|\psi_{a_1}(q_1)\rangle v_{\alpha_1}(q_1), \tag{15}$$

where

$$v_\alpha(q) = \langle\psi_a(q)|V_a\langle\alpha|\langle u_l(p)|A|\Phi\rangle. \tag{16}$$

Here

$$B = (1-\Lambda)^{-1},$$

with

$$\Lambda = \sum_\alpha{}' \int' dp A|u_l(p)\rangle|\alpha\rangle\{\omega_a(q)-1\}\langle\alpha|\langle u_l(p)|$$
$$-\left\{\sum_\alpha{}' \int'' dp + \sum_\alpha{}'' \int_0^\infty dp\right\} A|u_l(p)\rangle|\alpha\rangle G_{0,a}^{(2)}(q)t_a(q)\langle\alpha|\langle u_l(p)|. \tag{17}$$

Our method of perturbation iteration is to calculate B by the series expansion in powers of Λ. For the rest of this section, we write the perturbation formula.

Multiplying $\langle\psi_a(q)|V_a\langle\alpha|\langle u_l(p)|$ on both sides of Eq. (15), and using Eq. (16), we find

$$v_{\alpha_2}(q_2) = -\sum_{\alpha_2}{}' \int' dp_1 M_{\alpha_2 p_2, \alpha_1 p_1} v_{\alpha_1}(q_1), \tag{18}$$

with

$$M_{\alpha_2 p_2, \alpha_1 p_1} = \sum_{m=0}^\infty M^{(m)}_{\alpha_2 p_2, \alpha_1 p_1}$$
$$= \sum_{m=0}^\infty \langle\psi_{\alpha_2}(q_2)|V_{a_2}|\chi^{\alpha_2 p_2 (m)}_{\alpha_1 p_1}\rangle, \tag{19}$$

where

$$\chi^{\alpha_2 p_2 (0)}_{\alpha_1 p_1}(x) = A^{\alpha_2 p_2}_{\alpha_1 p_1}\psi_{a_1}(q_1, x) \tag{20}$$

and for $m \geqslant 1$

$$\chi^{\alpha_2 p_2 (m)}_{\alpha_1 p_1}(x) = \sum_{\alpha}{}' \int' dp A^{\alpha_2 p_2}_{\alpha p}[\omega_a(q)-1]\chi^{\alpha p (m-1)}_{\alpha_1 p_1} + \left(\sum_{\alpha}{}' \int'' dp + \sum_{\alpha}{}'' \int_0^{\infty} dp\right) A^{\alpha_2 p_2}_{\alpha p} G^{(2)}_{0,a}(q) \times t_a(q)\chi^{\alpha p (m-1)}_{\alpha_1 p_1}. \quad (21)$$

The operator $A^{\alpha_2 p_2}_{\alpha p}$ is defined by

$$A^{\alpha_2 p_2}_{\alpha p} F(x) = \langle \alpha_2 | \langle u_{l_2}(p_2) | A | u_l(p) \rangle | \alpha \rangle F(x), \quad (22)$$

where $F(x)$ is a function of x.

Starting from the basic Sturm-Liouville functions ψ_a, we compute the functions $\chi^{\alpha_2 p_2 (m)}_{\alpha_1 p_1}(x)$ by successive iterations using Eqs. (20) and (21). The matrix elements $M^{(m)}_{\alpha_2 p_2, \alpha_1 p_1}$ at each iteration are obtained by Eq. (19). The energy $|E|$, where Eq. (18) has a nontrivial solution, is the binding energy of ^{3}H. If we define a function $\chi^{\alpha p}_{\alpha_1 p_1}(x)$ by

$$\chi^{\alpha p}_{\alpha_1 p_1}(x) = \sum_{m=0}^{\infty} \chi^{\alpha p (m)}_{\alpha_1 p_1}(x), \quad (23)$$

the wave function $\phi_\alpha(x, y)$ in Eq. (11) is given by

$$\phi_\alpha(x,y) = -\int' dp u_l(p,y)\left(\psi_a(q,x)v_\alpha(q) + [\omega_a(q)-1]\sum_{\alpha_1}{}' \int' dp_1 \chi^{\alpha p}_{\alpha_1 p_1}(x) v_{\alpha_1}(q_1)\right) - \int'' dp u_l(p,y) G^{(2)}_{0,a}(q) t_a(q) \sum_{\alpha_1}{}' \int' dp_1 \chi^{\alpha p}_{\alpha_1 p_1}(x) v_{\alpha_1}(q_1), \quad (24)$$

for α belonging to the basic states, and

$$\phi_\alpha(x,y) = -\int_0^{\infty} dp u_l(p,y) G^{(2)}_{0,a}(q) t_a(q) \sum_{\alpha_1}{}' \int' dp_1 \chi^{\alpha p}_{\alpha_1 p_1}(x) v_{\alpha_1}(q_1), \quad (24')$$

for α outside the basic states. For the sake of simplicity, we write these two expressions in a unified manner:

$$\phi_\alpha(x,y) = \int dp u_l(p,y) \chi_\alpha(p,x), \quad (25)$$

which defines the function $\chi_\alpha(p, x)$.

III. PERTURBATION CALCULATION

In order to perform the iterations of Eq. (21), we need to compute a function $X^{\alpha p (m)}_{\alpha_1 p_1}(x)$ defined by

$$X^{\alpha p (m)}_{\alpha_1 p_1}(x) = [\omega_a(q)-1]\chi^{\alpha p (m-1)}_{\alpha_1 p_1}(x) \quad (26)$$

for a known function $\chi^{\alpha p (m-1)}_{\alpha_1 p_1}(x)$. This is done by solving the following Schrödinger-type differential equation which is equivalent to Eq. (26)[9]:

$$\left(-q^2 + \frac{d^2}{dx^2} + \frac{2}{x}\frac{d}{dx} - \frac{L(L+1)}{x^2} - V_a(x)\right) X^{\alpha p (m)}_{\alpha_1 p_1}(x) = V_a(x)\left(\chi^{\alpha p (m-1)}_{\alpha_1 p_1}(x) + \psi_a(q,x)\frac{1-\lambda_a(q)}{\lambda_a(q)} M^{(m-1)}_{\alpha p, \alpha_1 p_1}\right). \quad (27)$$

To solve this equation, we impose the boundary condition that the function $X^{\alpha p (m)}_{\alpha_1 p_1}(x)$ is regular at $x \to 0$ and exponentially decreasing at $x \to \infty$. The term $G^{(2)}_{0,a}(q) t_a(q)\, \chi^{\alpha p (m-1)}_{\alpha_1 p_1}(x)$ in Eq. (21) is calculated by solving an equation similar to Eq. (27) but without the term involving $\psi_a(q, x)$ on the right-hand side. The Sturm-Liouville function $\psi_a(q, x)$ is calculated by solving a differential equation that is equivalent to Eq. (3),

$$\left(-q^2 + \frac{d^2}{dx^2} + \frac{2}{x}\frac{d}{dx} - \frac{L(L+1)}{x^2} - V_a(x)/\lambda_a(q)\right)\psi_a(q,x) = 0. \quad (28)$$

In solving this equation, we impose the same boundary conditions that are imposed on Eq. (27).

For a given set of a and q, the solution of Eq. (28) satisfying these boundary conditions exists for enumerable infinite number of discrete values of $\lambda_a(q)$. The first Sturm-Liouville function that we use is the solution for the largest $\lambda_a(q)$ without node.

The operator $A^{\alpha_2 p_2}_{\alpha_1 p_1}$ defined by Eq. (22) is handled by the following formula[9,18]:

$$A^{\alpha_2 p_2 F^{\alpha_1}}_{\alpha_1 p_1}(x) = 2p_2 p_1 \int_{-1}^{1} du\, j_{L_2}(\lambda x)\Lambda_{p_2 p_1}(\alpha_2\alpha_1; u) \times \int_0^\infty x'^2 dx'\, j_{L_1}(\lambda_1 x') F^{\alpha_1}(x'). \tag{29}$$

The notation used in Eq. (29) is

$$u = \cos\theta_{\vec{p}_2 \times \vec{p}_1}$$

$$\vec{\lambda} = \vec{p}_2/2 + \vec{p}_1, \qquad \vec{\lambda}_1 = -(\vec{p}_2 + \vec{p}_1/2), \tag{30}$$

and

$$\Lambda_{p_2 p_1}(\alpha_2\alpha_1; u) = \sum_{\mathfrak{L}\mathcal{S}} C^{(\mathfrak{L}\mathcal{S})}_{\alpha_2\alpha_1} [(2l_1+1)/4\pi]^{1/2} \sum_{k\kappa} \langle L_2 k\, l_2 \kappa | \mathfrak{L}, k+\kappa\rangle \times \langle L_1 k+\kappa,\, l_1, 0 | \mathfrak{L}, k+\kappa\rangle Y^{k*}_{L_2}(\vec{\lambda}\cdot\hat{\vec{p}}_1) Y^{\kappa*}_{l_2}(\vec{p}\cdot\hat{\vec{p}}_1) Y^{k+\kappa}_{L_1}(\vec{\lambda}_1\cdot\hat{\vec{p}}_1), \tag{31}$$

where

$$C^{(\mathfrak{L}\mathcal{S})}_{\alpha_2\alpha_1} = 16\pi i^{l_2-l_1+L_2-L_1}[(2J_2+1)(2J_1+1)(2j_2+1)(2j_1+1)]^{1/2}(2\mathcal{S}+1) \begin{pmatrix} L_2 l_2 L \\ S_2\, \frac{1}{2}\, \mathcal{S} \\ J_2\, j_2 J_0 \end{pmatrix} \begin{pmatrix} L_1 l_1 L \\ S_1\, \frac{1}{2}\, \mathcal{S} \\ J_1\, j_1 J_0 \end{pmatrix} C^{I_2 I_1; T}_{S_2 S_1; \mathcal{S}}. \tag{32}$$

By the parity requirement, (l_2+L_2) and (l_1+L_1) are both even or both odd. As a result, the phase factor $i^{l_2-l_1+L_2-L_1}$ is real. The coefficient $C^{I_2 I_1; T}_{S_2 S_1; \mathcal{S}}$ in Eq. (32) is given by Table I.

The integration over x' in Eq. (29) for the asymptotic region (i.e., outside the potential range, $x_M < x < \infty$) is done analytically by making use of the asymptotic behavior of $F^{\alpha_1}(x')$, as described in Ref. 18. This is where the long-range nature of the particle exchange enters. Therefore, it is important to take the contribution of the asymptotic region into account accurately. The numerical integrations over u and x' (for $0 \leq x' < x_M$) in Eq. (29) require a careful treatment since they involve oscillatory functions $j_{L_2}(\lambda x)$ and $j_{L_1}(\lambda_1 x')$. The integrations are done with Simpson's method always using small enough mesh sizes equivalent to having at least 12 mesh points in one period of $\sin(\lambda x)$ or $\sin(\lambda_1 x')$. Since the remainder of the integrands is a slowly varying function of the arguments, an accurate interpolation on it at these finer mesh points is always possible.

TABLE I. The coefficient $C^{II_1; T=1/2}_{S\mathcal{S}_1; S_0}$ in Eq. (32). For $S_0 = \frac{3}{2}$ ($\frac{1}{2}$), this is the 2×2 (4×4) matrix.

(I,S) \ (I_1,S_1)	(0,1)	(1,1)
(0,1)	$-\frac{1}{2}$	$-\sqrt{3}/2$
(1,1)	$+\sqrt{3}/2$	$-\frac{1}{2}$

(I,S) \ (I_1,S_1)	(0,0)	(0,1)	(1,0)	(1,1)
(0,0)	$\frac{1}{4}$	$+\sqrt{3}/4$	$+\sqrt{3}/4$	$\frac{3}{4}$
(0,1)	$-\sqrt{3}/4$	$\frac{1}{4}$	$-\frac{3}{4}$	$+\sqrt{3}/4$
(1,0)	$-\sqrt{3}/4$	$-\frac{3}{4}$	$\frac{1}{4}$	$+\sqrt{3}/4$
(1,1)	$\frac{3}{4}$	$-\sqrt{3}/4$	$-\sqrt{3}/4$	$\frac{1}{4}$

IV. RESULT FOR CENTRAL S-WAVE POTENTIALS

For the purpose of testing the convergence property of our perturbation theory, first, we solve the bound state problem for purely central potentials. For the ^3S interaction, we use a regularized Yukawa potential with a soft core

$$V(^3S) = \hbar c[-p_1 e^{-p_2 x} + p_3 e^{-2p_2 x} - (p_3 - p_1) e^{-5p_2 x}]/x \tag{33}$$

with $\hbar c = 197$ MeV fm, $p_1 = 3.1344$, $p_2 = 1.5502$ fm^{-1}, and $p_3 = 7.4616$. In Eq. (33), x is given in units of

TABLE II. The ^3S phase shifts and the deuteron binding energy obtained by $V(^3S)$ of Eq. (33).

$E_{\rm Lab}$ (MeV)	25	95	150	210	330
Phase shift (degrees)	78.42	44.15	32.28	23.61	12.23

Deuteron binding energy: $|E_d| = 2.229$ MeV.

fm. This potential reproduces the two-nucleon $^3S_1$ data as shown in Table II. The potential (33) is similar to the Malfliet-Tjon potential,[6] but is regular at the origin, and is thus suitable for the performance of accurate numerical calculations. For the $^1S_0$ interaction $V(^1S)$ we use the RSC potential[5] with a cutoff mass of 30 times the pion mass to regularize the potential. More specifically, for $V(^1S)$, we replace all the Yukawa potential $e^{-n\rho}/\rho$ (where $\rho = \mu x$ with $\mu = m_\pi c/\hbar$), appearing in the RSC potential, by

$$Y(n, \kappa, \rho) = \frac{1}{\rho}\left[e^{-n\rho} - e^{-k\rho}\left(1 + \frac{\kappa^2 - n^2}{2\kappa}\rho\right)\right], \qquad (34)$$

where $\kappa = 30$. This regularization procedure is introduced by Green[24] and renders the potential highly regularized at the origin. The cutoff mass of $30m_\pi$ is large enough not to affect the $^1S_0$ phase shifts in any appreciable way, yet sufficient to regularize the potential.

In order to speed up the calculation, we set up an uneven x mesh by the following function from $x = 0$ to $x_M = 6$ fm:

$$x(t) = \frac{1}{12}t + 10e^{-0.8(9-t)} - 4.742\,63e^{-1.2(9-t)} - 0.007\,369\,1. \qquad (35)$$

This function is shown in Fig. 1. The t-mesh size used is 0.3 fm and the total number of t mesh is 30, ranging from $t = 0$ to 9 fm. We used the Numerov method for the numerical integration of Eqs. (27) and (28).

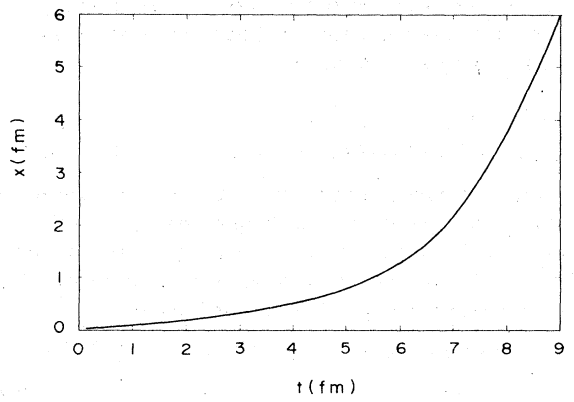

FIG. 1. The function $x(t)$ of Eq. (35) used to set up an uneven x mesh. The equidistant mesh size used for t is 0.3 fm ranging from $t = 0$ to 9 fm.

For these two-nucleon potentials, the Sturm-Liouville functions are obtained by solving the differential equation (28). In Table III, we present the first ($n = 1$) eigenvalues $\lambda_a(q)$ for $a = {}^3S$ and ^1S. The value of q where the eigenvalue is equal to 1 corresponds to the deuteron binding energy. In Table III, we also show the second and the third ($n = 2$ and 3) eigenvalues for the ^3S state.

Since the function ψ_a is normalized as Eq. (4), it is apparent from Table III that we need to include only the first Sturm-Liouville function in the unperturbed term of Eq. (6), bringing all other terms into $g_a(q)$ to be treated as the perturbation. Indeed, our preliminary calculations show that the inclusion of the second and the third eigenfunctions in the unperturbed part does not improve the convergence appreciably but merely increases the consumption of the computer time and the memory space. Also, it is seen that the value of q_M, up to which the separation (6) is made for $G^{(2)}_{0,a}(q)$, may be chosen to be 0.8 fm^{-1}, for example. These are rather fortunate situations peculiar to the two-nucleon interaction in general, not just for the particular potentials we have chosen.

For the basic momentum [i.e., $(m|E|)^{1/2}/\hbar \leq q \leq q_M$], we use six equidistant p-mesh ranging from $p = 0$ to p_M. Here, p_M corresponds to q_M by the relation of q and p given in Sec. I. We take 0.750 fm^{-1} as the value of p_M, so that the p-mesh size is 0.125 fm^{-1}. (For $|E| = 6.70$ MeV, 0.75 fm^{-1} for p_M corresponds to 0.7642 fm^{-1} for q_M.) Above p_M, we use six p-mesh points of 0.2 fm^{-1} intervals up to 1.95 fm^{-1}. This will be referred to as "the standard p mesh."

The method of calculating the three-body bound state has already been explained. We look for the energy $|E|$ at which Eq. (18) is satisfied. In the discretized form, it can be written as

$$v_i = -\sum_{j=1}^{N} M_{ij} w_j v_j \quad (i = 1, 2, \ldots, N), \qquad (36)$$

TABLE III. The eigenvalue $\lambda_n(q)$ of the Sturm-Liouville function for the central potentials of Sec. IV.

q (fm^{-1}) \ $\lambda_n(q)$	$^3S_1$ state $n=1$	$n=2$	$n=3$	$^1S_0$ state $n=1$
0.1	1.2344	0.1691	0.063 17	0.8106
0.2	1.0505	0.1582	0.060 59	0.7176
0.3	0.9046	0.1484	0.058 17	0.6408
0.4	0.7868	0.1396	0.055 91	0.5764
0.5	0.6906	0.1315	0.053 79	0.5216
0.6	0.6109	0.1242	0.051 80	0.4745
0.7	0.5442	0.1174	0.049 93	0.4337
0.8	0.4879	0.1113	0.048 16	0.3981
0.9	0.4398	0.1056	0.046 50	0.3667
1.0	0.3986	0.1004	0.044 92	0.3390

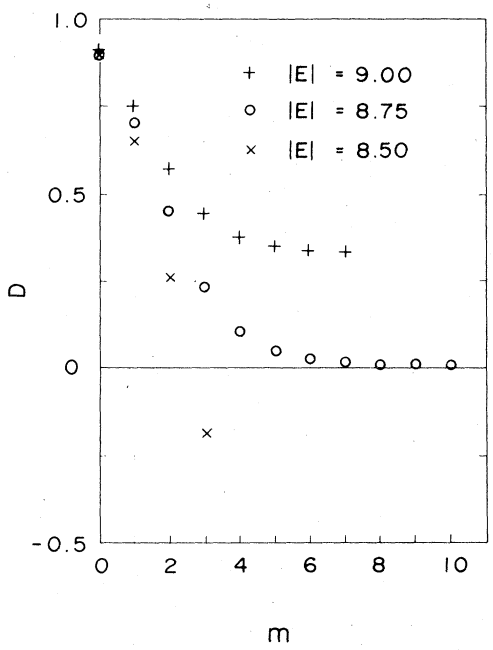

FIG. 2. Typical example of convergence for the central potentials of Sec. IV. The residual D is plotted at each order of iteration m for each value of $|E|$ shown in the figure.

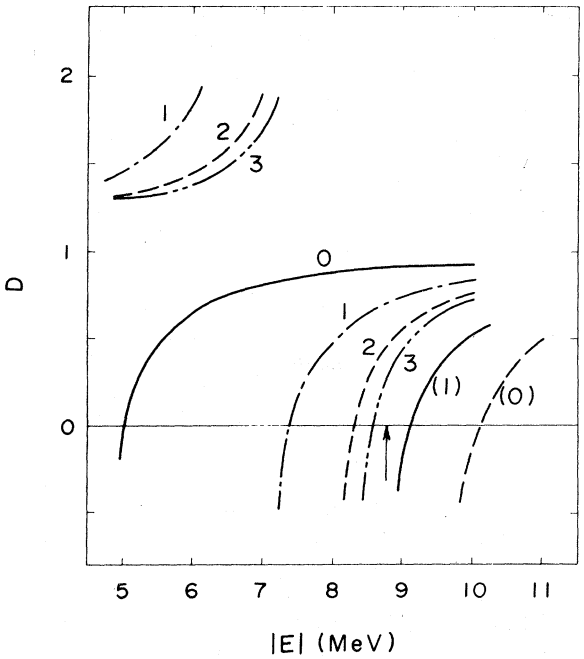

FIG. 3. The residual D as a function of $|E|$ at each order of iteration for the central potentials of Sec. IV. The numbers on the curves indicate the order of iteration. Curves with numbers not enclosed in parentheses represent the calculated results with the standard p mesh for which both the left and the right branches are shown. Curves with numbers inside parentheses represent the calculated values with 10 equal mesh up to $p_M = 1.6$ fm^{-1}, for which only right branches are illustrated.

where N is the dimensionality of the basic vector $\vec{v}$, which is given by the number of two-body states times the number of basic p mesh. This is the dimensionality of our Faddeev equation written in a matrix form. Since the singlet and the triplet two-body states constitute a different basis, the dimensionality of our problem is 12 ($=2\times6$) for the "standard p mesh". In Eq. (36), M_{ij} is the matrix element and w_j is the weight of the p quadrature. We use Simpson's method. For a chosen value of $|E|$, we compute M_{ij} as explained in Sec. III. Assuming $v_1 = 1$, we solve Eq. (36) for v_i ($i \geqq 2$). The resulting values of v_i ($i \geqq 2$) are put back in the first equation ($i = 1$) of Eq. (36). The residual (the difference between the left-hand side and the right-hand side) of this equation is denoted by D. The value of $|E|$ at which D converges to zero gives ^{3}H binding energy. In Fig. 2, we show typical examples of the values of D computed using the standard p mesh, where we have chosen as the number 1 component ($i = 1$) in Eq. (36) to be the $^1S_0$ component at the first p mesh. As can be seen

TABLE IV. The values of the residual D for the central potentials of Sec. IV for $p_M = 0.75$ fm^{-1} and 0.85 fm^{-1} as a function of the order of iteration m and the trial values of $|E|$.

m \ E (MeV)	$p_M = 0.75$ fm^{-1} 8	8.5	8.75	$p_M = 0.85$ fm^{-1} 9	8.75
0	0.872	0.893	0.901	0.909	0.828
1	0.466	0.649	0.703	0.743	0.424
2	−1.16	0.258	0.450	0.567	0.142
3	52.3	−0.186	0.232	0.438	0.0401
4			0.105	0.372	0.0076
5			0.0471	0.343	−0.0016
6			0.0241	0.333	−0.0041
7			0.0155	0.329	
8			0.0123		
9			0.0111		
10			0.0106		

from this figure, D is quite sensitive to the choice of $|E|$ and converges within five iterations. The value of $|E|$ at which D converges to zero is 8.75 MeV. In Table IV, we give the values of D corresponding to Fig. 2. Since the residual D is so sensitive to the choice of $|E|$, we consider $|E| = 8.75$ MeV to be close enough to be called the binding energy within the accuracy of our numerical calculation.

In Fig. 3, we show D as a function of $|E|$ at each iteration. In general, there occur two branches in D. Only the right branch can cut the abscissa at the value of $|E|$ where Eq. (18) is satisfied within the order iteration shown on the curve. The limiting value of $|E| = 8.75$ MeV is indicated by an arrow. All these calculations are done with the standard p mesh.

The result of the perturbational calculation should not depend on the choice of q_M (or, equivalently, p_M). To see this is indeed the case, we next compute D at $|E| = 8.75$ MeV with 6 equal intervals up to $p_M = 0.85$ fm^{-1} and 6 equal intervals of 0.2 fm^{-1} beyond that. The results are also shown in Table IV. Considering the sensitivity of D to $|E|$, we accept the value of 8.75 MeV as the binding energy in this case too. To see the behavior of D when p_M is drastically different from the standard case, we repeat the calculation using ten equal intervals up to $p_M = 1.6$ fm^{-1}. The results are shown in Table V, and also in Fig. 3 by the curves with numbers inside parentheses. (Only the right branches are drawn for the calculated results with this p mesh.) Apparently, again we find $|E| = 8.75$ MeV as the binding energy. We remark that the perturbation acts attractively (toward stronger binding compared to the 0th order around 5 MeV) when $p_M = 0.75$ fm^{-1}, and repulsively (toward less binding compared to the 0th order aroung 10 MeV) when $p_M = 1.6$ fm^{-1}. Despite this and also the different choices of p mesh, it is gratifying to find the same binding energy.

V. RESULTS FOR THE RSC POTENTIAL

Here, we present the result of the calculation for the RSC potential.[5] In our calculation, only the $^1S_0$ and the $^3S_1 + {}^3D_1$ states for a two-body system and the s state for the spectator are taken into account.

TABLE V. The value of D for $p_M = 1.60$ fm^{-1} for the central potentials of Sec. IV.

m \ E (MeV)	8.75	9	10	11
0	4.58	17.2	−0.121	0.494
1	−0.159		0.532	
2	+0.0461			
3	−0.0034			

As the RSC potential has a $1/r$ singularity, we must regularize it to obtain the solutions of Eqs. (27) and (28) accurately near the origin. (Otherwise, we have to make a power series expansion of the wave function in terms of the distance near the origin. However, this is extremely cumbersome,[25] and impractical.) As in Sec. IV for $V(^1S_0)$, the regularization is done by introducing a heavy cutoff mass (50 times the pion mass), which does not affect the deuteron properties and the phase shifts as well as the off-shell properties in any significant way. Thus in the RSC potential, we replace the Yukawa function $e^{-n\rho}/\rho$ by $Y(n, \kappa, \rho)$ of Eq. (34) everywhere except in the following two terms in the tensor part. We replace $(1 + 3/\rho + 3/\rho^2)e^{-\rho}/\rho$ by

$$\left(1 + \frac{3}{\rho} + \frac{3}{\rho^2}\right)\frac{e^{-\rho}}{\rho} - \left[\frac{3\kappa^2 - 1}{2} + \frac{3\kappa}{\rho} + \frac{3}{\rho^2} + \frac{\kappa(\kappa^2 - 1)}{2}\rho\right]\frac{e^{-\kappa\rho}}{\rho}, \tag{37}$$

which vanishes at the origin, and $(12/\rho + 3/\rho^2)e^{-4\rho}/\rho$ by

$$\left(\frac{12}{\rho} + \frac{3}{\rho^2}\right)\frac{e^{-4\rho}}{\rho} - 16\left[\frac{3\bar{\kappa}^2 - 1}{2} + \frac{3\bar{\kappa}}{\xi} + \frac{3}{\xi^2} + \frac{\bar{\kappa}(\bar{\kappa}^2 - 1)}{2}\xi\right]\frac{e^{-\kappa\rho}}{\rho} - 16Y(4, \kappa, \rho), \tag{38}$$

which becomes flat at the origin. These are also the double cutoff procedures of Green.[24] Here $\kappa = 50$, $\bar{\kappa} = \kappa/4$, and $\xi = 4\rho$. As in Eq. (34), $\rho = (m_\pi c/\hbar)x$.

The eigenvalues $\lambda_a(q)$ of the first Sturm-Liouville functions for $^3S_1 + {}^3D_1$ and $^1S_0$ are shown in Fig. 4. The value of $q = 0.23140$ fm^{-1} for the $^3S_1 + {}^3D_1$ state at which the eigenvalue is equal to 1 corresponds to the deuteron binding energy

$$|E_d| = \frac{\hbar^2}{m}q^2 + 41.47q^2 = 2.221 \text{ (MeV)}. \tag{39}$$

In Fig. 4, the second eigenvalue of the $^3S_1 + {}^3D_1$ state are also shown by the dashed curve. As in Sec. IV, we will not use the second and higher Sturm-Liouville functions as the unperturbed part.

We use the standard p mesh and the uneven x mesh explained in Sec. IV. Examples of convergence are shown in Fig. 5, in which the residual D is shown for each order of iteration for a few values of $|E|$ indicated in the figure. Here, we use as the number 1 component in Eq. (36) the $^3S_1 + {}^3D_1$ component at the first p mesh. The value of $|E|$ at which D converges to zero is 6.617 MeV. This is the ^{3}H binding energy. The (unnormalized) basic vector $\tilde{\mathbf{v}}$ is shown in Fig. 6.

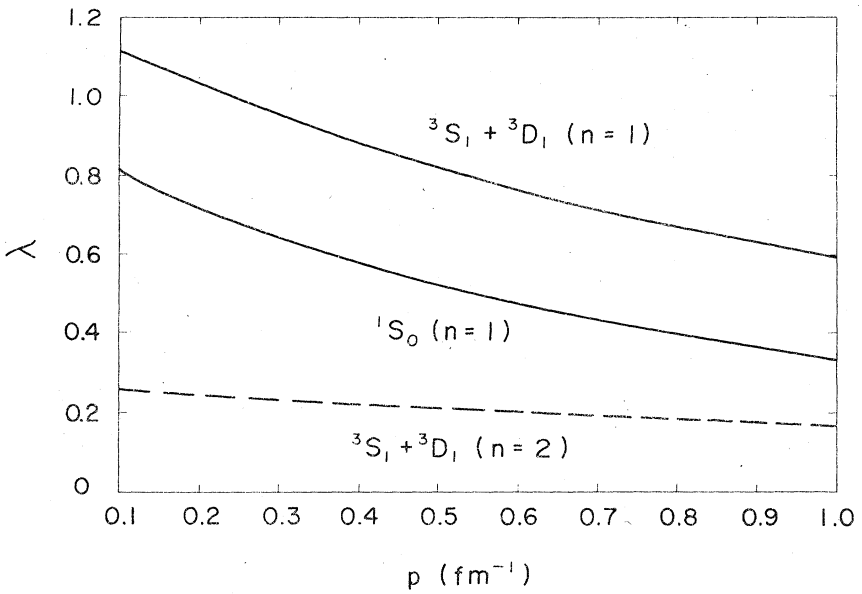

FIG. 4. The first ($n = 1$) and the second ($n = 2$) eigenvalues λ of the Sturm-Liouville functions for the RSC potential.

The basic vector $\vec{v}$ thus obtained is used in Eqs. (24) and (25) to find $\phi_\alpha(x, y)$, from which we construct the triton wave function as given by Eqs. (9), (10), and (11). In terms of $\psi^{S(A)}$ of Eq. (11), the one-body charge form factors F_{ch} (^{3}He) and F_{ch}(^{3}H) are given by the formulas in the appendix.[10]

As the nucleon charge form factors $F^p_{ch}(q)$ and $F^n_{ch}(q)$, (q = the momentum transfer), we use the analytic expression given by Janssens *et al.*[26] In Fig. 7, we show the charge form factors together with the experimental data from Refs. 27 and 28. Our $|F_{ch}(^3\text{He})|$ has a dip at $q^2 \sim 16$ fm^{-2} and its second maximum is approximately an order of magnitude too low compared to the data. For the basic states adopted in the present paper, $F_i^{AA} = F_i(^1S_0, l=0)$, $F_i^{SS} = F_i(^3S_1, l=0) + F_i(^3D_1, l=0)$ for $i = 1, 2, 3$, and 4, and $F_i^{AS} = F_i^{SA} = 0$ for $i = 1$ and 2. Also, $F_4^{AS} = -F_4^{SA} = F_4(^1S_0, {}^3S_1)$. In Figs. 8 and 9, we show the contribution from each component.

In Figs. 10 and 11, we show typical behaviors of the wave function $x\chi_\alpha(p, x)$ for the three components $^1S_0$, $^3S_1$, and $^3D_1$ as functions of x at $p = 0.25$ fm^{-1} and as functions of p at $x = 1.27$ fm (before the over-all normalization). [The function $\chi_\alpha(p, x)$ is defined by Eq. (25).] Figure 10 shows that there is a node at $x \sim 0.5$ fm for each of the $^1S_0$ and the $^3S_1$ components, while there is no node for the $^3D_1$ component. Although we have used different formulas to compute the function $x\chi_\alpha(p, x)$ for $p \leqslant p_M$ and

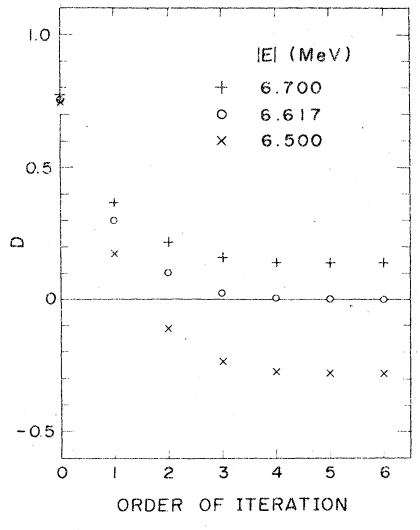

FIG. 5. Typical examples of convergence for the RSC potential. See the caption of Fig. 2.

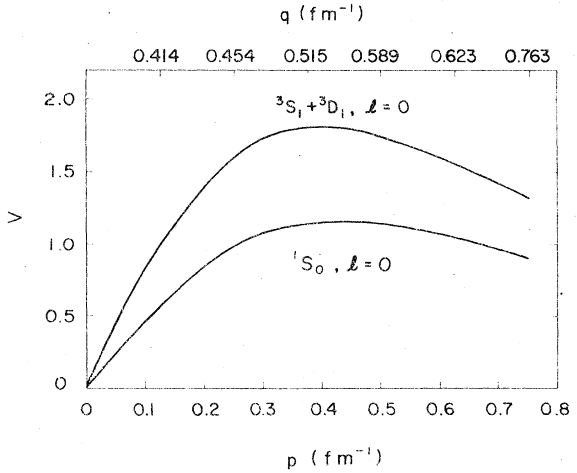

FIG. 6. The basic vectors $v_\alpha(q)$ of Eq. (16) at $|E| = 6.617$ MeV, before the overall normalization.

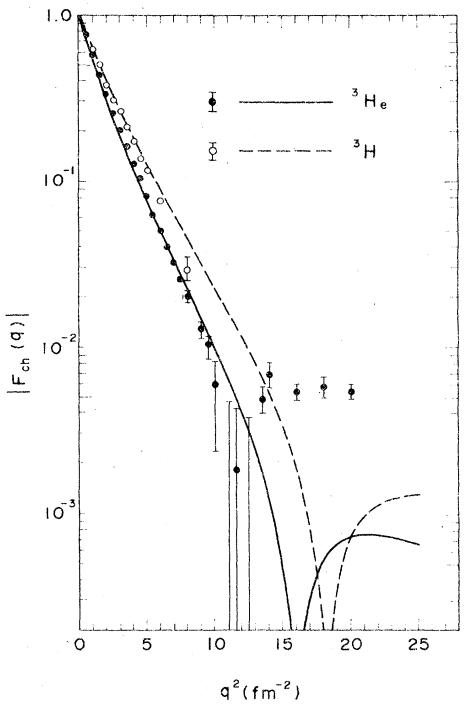

FIG. 7. The one-body charge form factors of ^{3}He (solid curve). The experimental values are taken from Refs. 27 and 28.

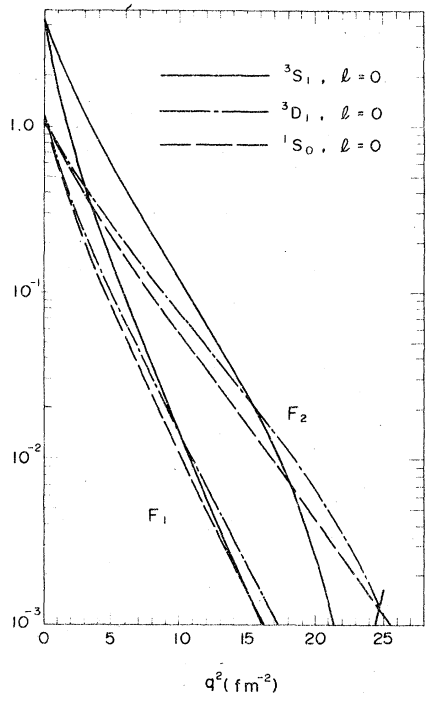

FIG. 8. The components F_1 and F_2 appeared in Eq. (A3) (before the overall normalization).

for $p > p_M$, Fig. 11 shows that this function is smoothly connected at $p = p_M$, as it should be. It is also seen from Fig. 11 that the maximum value of the spectator momentum used in the standard p mesh ($p_{max} = 1.95$ fm^{-1}) is sufficiently large.

After performing the integration over p in Eq. (25), the function $xy\phi_\alpha(x,y)$ is obtained for three components. The integration over p in Eq. (25) requires some care since $u_l(p,y)$ is an oscillating function. The contribution from the ith p interval (from p_{i-1} to p_i) of the standard p mesh is carried out by Simpson's method using a finer p-mesh size Δp so chosen that $\Delta p \cdot y$ is not greater than 0.5 (which is equivalent to having at least 12 mesh points in one period of $\sin py$). This necessitates an interpolation on $\chi_\alpha(p,x)$ over p. This is done quadratically using the values of $\chi_\alpha(p_i,x)$ at the nearest three p_i's, which is accurate enough since $\chi_\alpha(p,x)$ is a slowly varying function of p. Then the contributions from all p intervals from $i=1$ to 12 thus obtained are added to find $xy\phi_\alpha(x,y)$.

The $^1S_0$ and the $^3S_1$ components (with $l=0$) are shown in Fig. 12 as functions of x at $y=0.5$, 2.0, and 6.0 fm (before the overall normalization). The node of the function $x\chi_\alpha(p,x)$ at around $x=0.5$ fm still persists in the function $xy\phi_\alpha(x,y)$. This behavior of the radial wave function has not been reported so far. The presence of this node suggests that it is almost impossible to perform an accurate numerical calculation of the Faddeev equation in the manner of expanding it by a complete orthonormal set of functions, say, that of the harmonic oscillator functions.

The y dependence of $xy\phi_\alpha(x,y)$ is shown in Fig. 13. There is no node as a function of y in any component. Also, the function $xy\phi_\alpha(x,y)$ is surprisingly long ranged in the y direction.

In order to get some idea for the origin of the node in the $^1S_0$ and the $^3S_1$ components, we show by the solid curve of Fig. 14, the function $x\chi^{\alpha\, p(0)}_{\alpha_1 p_1}(x)$ of Eq. (20) for $\alpha=\alpha_1=(^1S_0, l=0)$ with $p=0.125$ fm^{-1} and $p_1=0.750$ fm^{-1}. The fact that this function starts out linearly at $x=0$ is due to the spherical Bessel function $j_0(\lambda x)$ in Eq. (29). In Eq. (27), this function multiplied by the potential $V_a(x)$ is used in the inhomogeneous term. The terms on the right-hand side of Eq. (27) are exactly a consequence of the particle exchange characteristic of the Faddeev equation. In Fig. 14, we show $xV_a(x)\chi^{\alpha\, p(0)}_{\alpha_1 p_1}(x)$ by the dashed curve. The linear behavior of the function $x\chi^{\alpha\, p(0)}_{\alpha_1 p_1}(x)$ near $x=0$ multiplied by the strong soft-core yields a very narrow peak within the core radius. This property of the source term in Eq. (27) is reflected to the solution of this equation. Thus we conclude that the strong soft core of the RSC potential coupled with the particle exchange effect of the Faddeev

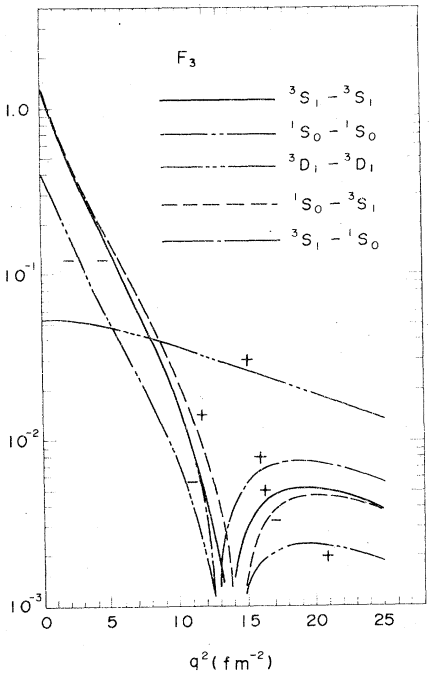

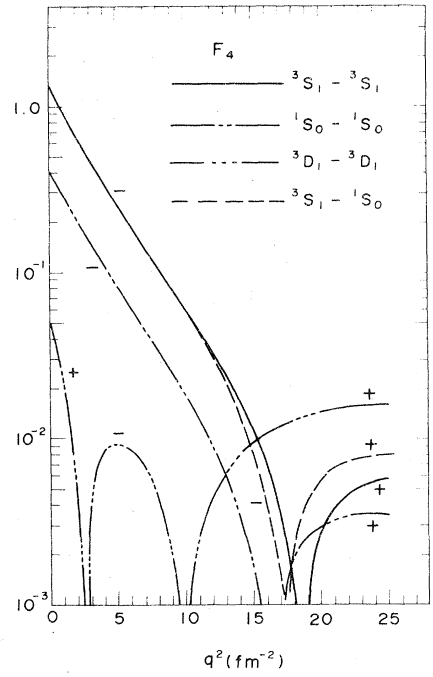

FIG. 9. The components F_3 and F_4 appeared in Eq. (A3) (before overall normalization). The plus and minus signs indicate the signs of the values of F_3 and F_4.

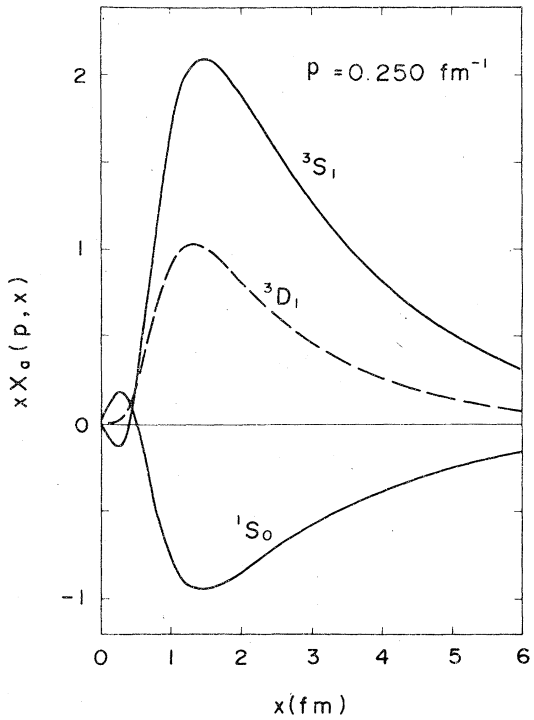

FIG. 10. $x\chi_\alpha(p,x)$ defined by Eq. (26) as a function of x at $p=0.25$ fm^{-1}.

equation gives rise to the node near the origin of the radial wave function.

Throughout the calculation, we have so far used the cut-off parameter $\kappa=50$ (~7,000 MeV) in Eqs. (37) and (38). The effect of introducing the cut-off may be judged from the values of the deuteron binding energy $|E_d|$ and the ^{3}H binding energy $|E|$ obtained by varying the values of κ, as shown in Table VI. Apparently, $\kappa=20$ is too small having a marked effect on $|E_d|$, but $\kappa=30$ is already large enough. The resulting charge form factors for $\kappa=30$ are also very close to those of $\kappa=50$.

VI. SUMMARY AND CONCLUSION

The perturbation-iteration calculation of the ^{3}H bound state is carried out on the Faddeev equation, utilizing the first Sturm-Liouville functions

TABLE VI. The effect of the cut-off variation on the deuteron and the triton binding energies, $|E_d|$ and $|E|$, respectively.

κ	20	30	35	40	50	70
$\|E_d\|$	2.468	2.236	2.225	2.222	2.221	2.221
$\|E\|$	...	6.68	6.64	6.62	6.62	6.62

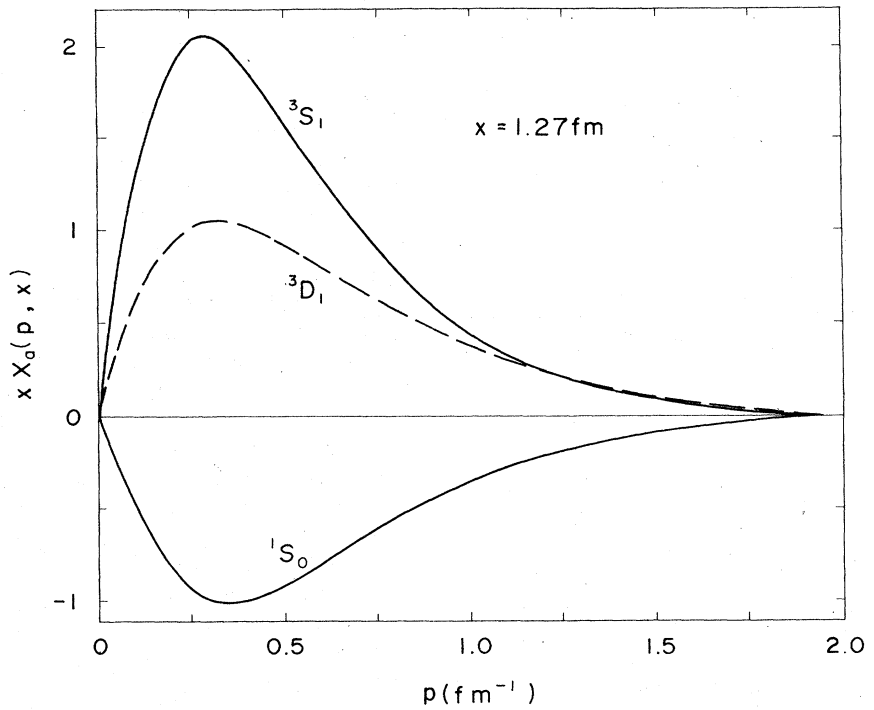

FIG. 11. $x\chi_\alpha(p,x)$ as a function of p at $x=1.27$ fm.

for the $^1S_0$ and the $^3S_1+^3D_1$ two-body states as the basis. The calculation is performed exactly in coordinate space. Using purely central s-wave potentials for the ^1S and the ^3S states as an example, the convergence property of our perturbation treatment is investigated in detail, and it is proved to be quite satisfactory.

As an example of the realistic two-nucleon interactions, the RSC potential is used to calculate the ^{3}H binding energy and the one-body charge form factors of ^{3}He and ^{3}H. The three-body states included are the lowest partial waves, consisting of the $^1S_0$ and the $^3S_1+^3D_1$ two-body states with the third particle in the s-state rela-

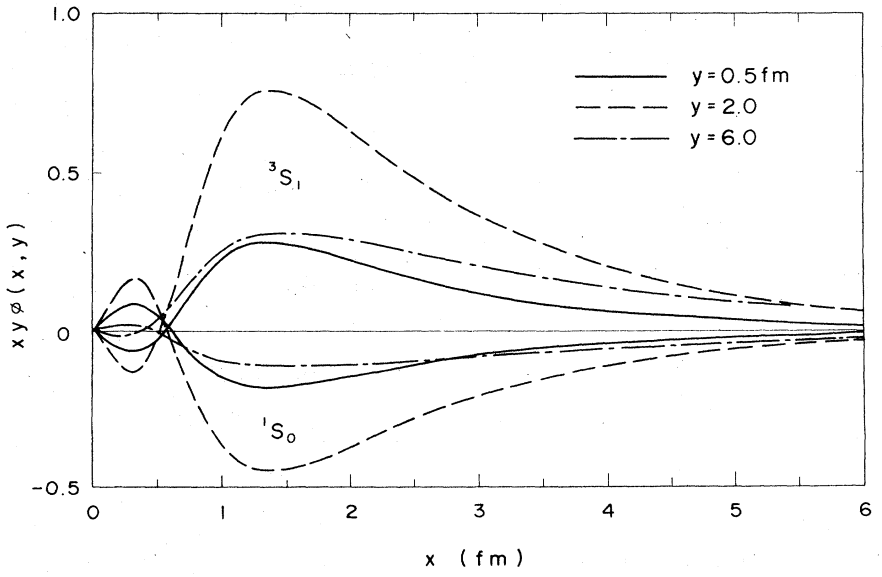

FIG. 12. $xy\phi_\alpha(x,y)$ of Eq. (26) as a function of x at $y=0.5$, 2.0, and 6.0 fm.

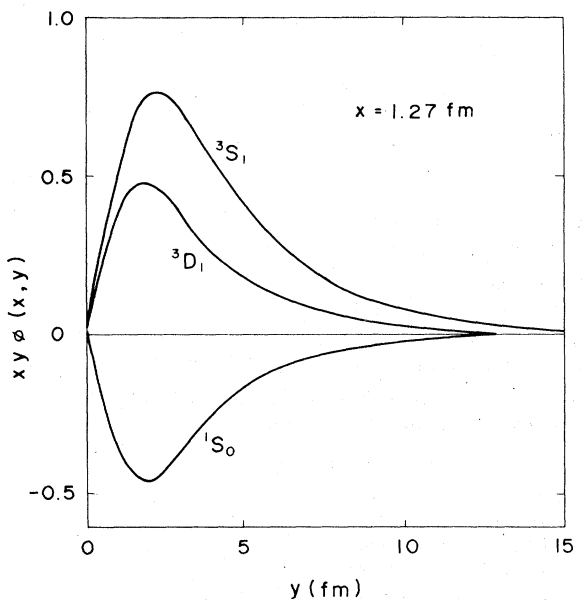

FIG. 13. $xy\phi_\alpha(x,y)$ as a function of y at $x=1.27$ fm.

tive to the center of the two-body pair.

The ^{3}H binding energy is found to be $|E| = 6.62$ MeV, fairly close to the values obtained by Malfliet and Tjon (6.4 ± 0.5 MeV),[6] Harper, Kim and Tubis (6.7 MeV),[7] Brandenburg, Kim, and Tubis (6.98 MeV),[7] and Gignoux and Lavern (7.0 MeV).[8] As the probability of the S, S' and D states, we get the following values: $P(S) = 90.28\%$, $P(S') = 1.70\%$ and $P(D) = 8.02\%$. These values are very close to the values obtained by other authors. We also repeated the calculation by adding the component in which the spectator particle is in the d-state. However, the binding energy of ^{3}H is increased only as much as 0.05 MeV.

The ^{3}He charge form factor turns out to have a dip at $q^2 \sim 16$ fm^{-2} with the height of the second peak an order of magnitude too low.

Each of the Faddeev components for the $^1S_0$ and the $^3S_1$ components has a node at around $x \sim 0.5$ fm as functions of x. No such node is found in the $^3D_1$ component. As functions of y, all these components do not have any node, but extend to large distances. The nodes in the $^1S_0$ and the $^3S_1$ components are attributed to the presence of the strong soft-core in the RSC potential coupled with the particle exchange terms in the Faddeev equation.

Note added in proof. The charge form factors reported at the Graz conference [*Few Body Systems and Nuclear Forces I*, edited by H. Zingl *et al.* (Springer, Berlin, 1978), p. 159] are incorrect. The charge form factors in the present paper are correct.

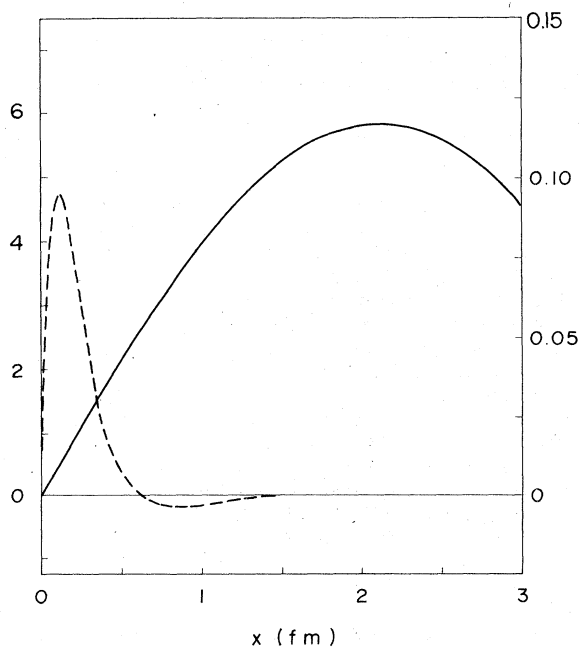

FIG. 14. $x\chi^{\alpha\ p}_{\alpha_1 p_1}{}^{(0)}(x)$ of Eq. (20) is given by the solid curve with the right scale for $\alpha = \alpha_1 = (^1S_0, l=0)$ with $p = 0.125$ fm^{-1} and $p_1 = 0.750$ fm^{-1} of the standard p mesh. $xV_a(x)\chi^{\alpha\ p}_{\alpha_1 p_1}{}^{(0)}(x)$ is also shown by the dashed curve with the left scale.

We would like to thank the Research Center for Nuclear Physics at Osaka University and the National Laboratory for High Energy Physics for their generous support in the use of their computers. We also would like to thank Dr. S. Shioyama for performing the computations necessary to prepare Fig. 3 at the Engineering Computation Consultant Co. Ltd., Tokyo. The part of the calculations for the RSC potential with the $l=2$ component was carried out at the Computing Center at Osaka University. We acknowledge Miss Y. Goto at the center for her valuable assistance in this phase of the work. This work was supported in part by the Japan Society for Promotion of Science under Grant No. 6R-036.

APPENDIX

The one-body charge form factors are given by

$$2F_{\rm ch}(^3{\rm He}) = F^p_{\rm ch}(3F_a + F_b) + 2F^n_{\rm ch}F_b, \tag{A1}$$

$$F_{\rm ch}(^3{\rm H}) = F^n_{\rm ch}(3F_a + F_b) + 2F^p_{\rm ch}F_b, \tag{A2}$$

where $F^p_{\rm ch}(q)$ and $F^n_{\rm ch}(q)$ are the nucleon charge form factors, q being the momentum transfer. In Eqs. (A1) and (A2), F_a is given by[10]

$$F_a(q) = F_1^{SS} + \tfrac{1}{2}F_2^{SS} - 2F_3^{SS} + \tfrac{1}{2}F_4^{SS} + \tfrac{3}{2}(F_2^{AA} - F_4^{AA}) + \sqrt{3}\,(\epsilon F_2^{SA} - 2F_3^{SA} - \epsilon F_4^{SA}), \tag{A3}$$

with $\epsilon = 1$. F_b is also given by an expression simi-

lar to Eq. (A3) but with $\epsilon = -1$ and suffixes S and A interchanged throughout. In Eq. (A3), there appear four kinds of form factors defined by

$$F_1^{uv} = \int e^{i\vec{q}\cdot\vec{r}_3} \langle \psi^u(12,3) | \psi^v(12,3) \rangle d^3r_i, \tag{A4}$$

$$F_2^{uv} = \int e^{i\vec{q}\cdot\vec{r}_3} \langle \psi^u(31,2) | \psi^v(31,2) \rangle d^3r_i, \tag{A5}$$

$$F_3^{uv} = \int e^{i\vec{q}\cdot\vec{r}_3} \langle \psi^u(12,3) | \psi^v(31,2) \rangle d^3r_i, \tag{A6}$$

$$F_4^{uv} = \int e^{i\vec{q}\cdot\vec{r}_3} \langle \psi^u(31,2) | \psi^v(23,1) \rangle d^3r_i, \tag{A7}$$

where $u = S$ or A and $v = S$ or A. ψ^S and ψ^A are given by Eq. (11). From the definitions it is obvious that

$$F_1^{uv} = F_1^{vu} \text{ and } F_2^{uv} = F_2^{vu}. \tag{A8}$$

Also,

$$F_4^{uv} = \epsilon F_4^{uv}, \tag{A9}$$

where $\epsilon = +1$ if $u = v$ and $\epsilon = -1$ if $u \neq v$. The last relation provides a nice check on the numerical accuracy.

We compute F_i^{uv} $(i = 1, 2, 3, 4)$ by taking the average over the magnetic quantum number M_0 of the total angular momentum J_0. The detailed expressions for $\langle F_i^{uv} \rangle$ and the method of actual calculation are found in Refs. 10 and 11.

[1] L. M. Delves and A. C. Phillips, Rev. Mod. Phys. 41, 497 (1969); L. M. Delves, Adv. Nucl. Phys. 5, 1 (1973); Y. E. Kim and A. Tubis, Annu. Rev. Nucl. Sci. 24, 69 (1974); J. S. Levinger, in *Springer Tracts in Modern Physics* (Springer, New York, 1974), Vol. 71.

[2] M. A. Hennell and L. M. Delves, Nucl. Phys. A246, 490 (1975). Previous calculations of the three-nucleon bound state with the RSC potential are found in this reference.

[3] L. D. Faddeev, *Mathematical Aspects of the Three-Body Problems in Quantum Scattering Theory*, translated from Russian, the Israel Program of Scientific Translations (Davey, New York, 1965).

[4] T. A. Osborn, J. Math. Phys. 14, 373 (1973); 14, 1485 (1973).

[5] R. V. Reid, Ann. Phys. (N.Y.) 50, 411 (1968).

[6] R. A. Malfliet and J. A. Tjon, Ann. Phys. (N.Y.) 61, 425 (1970).

[7] E. P. Harper, Y. E. Kim, and A. Tubis, Phys. Rev. Lett. 28, 1533 (1972); R. A. Brandenburg, Y. E. Kim, and A. Tubis, Phys. Rev. C 12, 1368 (1975).

[8] C. Gignoux and A. Lavern, Phys. Rev. Lett. 29, 436 (1972); A. Lavern and C. Gignoux, Nucl. Phys. A203, 597 (1973).

[9] T. Sasakawa, T. Sawada, and S. Shioyama, Sci. Rep. Tohoku Univ. Ser. 1, LX, 124 (1977).

[10] T. Sasakawa and T. Sawada, Sci. Rep. Tohoku Univ. Ser. 1, LXI, 47 (1978).

[11] T. Sasakawa and T. Sawada, Sci. Rep. Tohoku Univ. Ser. 1, LXI, 70 (1978). The programming for the present calculation is given in this reference.

[12] A. J. Dragt, J. Math. Phys. 6, 533 (1965); W. Zickendraht, Ann. Phys. (N.Y.) 35, 18 (1965); Yu. A. Simonov, Yad. Fiz. 3, 630 (1966) [Sov. J. Nucl. Phys. 3, 461 (1966)]; A. M. Badalyan and Yu. A. Simonov, Yad. Fiz. 3, 1032 (1966) [Sov. J. Nucl. Phys. 3, 755 (1966)]; Yu. A. Simonov and A. M. Badalyan, Yad. Fiz. 5, 88 (1967) [Sov. J. Nucl. Phys. 5, 60 (1967)]; V. V. Pustovalov and Yu. A. Simonov, Zh. Eksp. Teor. Fiz. 51, 345 (1966) [Sov. Phys.-JETP 24, 230 (1967)]; B. M. Dzyuba, V. V. Pustovalov, V. F. Rybachenko, A. A. Sadovoi, and V. D. Efros, Yad. Fiz. 13, 22 (1971) [Sov. J. Nucl. Phys. 13, 12 (1971)]; J. Revai and J. Raynal, Nuovo Cimento 68A, 612 (1970); J. Raynal, Nucl. Phys. A202, 631 (1973), Phys. Lett. 45B, 89 (1973); M. Fabre de la Ripelle, C. R. Acad. Sci. (Paris) 269, 1070 (1969); 273, 1007 (1971); 276, 961 (1973); Yad. Fiz. 13, 495 (1971) [Sov. J. Nucl. Phys. 13, 279 (1971)], Fizika 4, 1 (1972); M. Beinar and M. Fabre de la Ripelle, Nuovo Cimento Lett. 1, 584 (1971); M. J. Englefield, Nucl. Phys. A181, 305 (1972); J. Bruinsma and R. van Wageningen, Phys. Lett. 44B, 231 (1973).

[13] E. O. Alt, P. Grassberger, and W. Sandhas, Nucl. Phys. B2, 167 (1967); V. F. Kharchenko and N. M. Petrov, Nucl. Phys. A137, 417 (1967); V. F. Kharchenko and S. A. Strozenko, *ibid.* A137, 437 (1969); J. S. Ball and D. Y. Wong, Phys. Rev. 169, 1362 (1968); T. Sasakawa, Nucl. Phys. A160, 321 (1971).

[14] J. J. Benayoun and C. Gignoux, Nucl. Phys. A190, 419 (1972).

[15] A. D. Jackson, A. Lande, and P. U. Sauer, Phys. Lett. 35B, 365 (1971); 36B, 1 (1971); Nucl. Phys. A246, 490 (1975); W. Glöckle and R. Offermann, Phys. Rev. C 16, 2039 (1977); P. Nunberg, D. Prosperi, and E. Pace, Nucl. Phys. A258, 58 (1977).

[16] L. M. Delves, in *Few Body Problems in Nuclear and Particle Interactions*, edited by R. J. Slobodrian *et al.* (Les Press de Univ. Laval, Quebec, 1975), p. 446.

[17] T. Sasakawa and T. Sawada, Prog. Theor. Phys. Suppl. 61, 1 (1977).

[18] T. Sasakawa and T. Sawada, Prog. Theor. Phys. Suppl. 61, 61 (1977).

[19] T. Sasakawa, T. Sawada, and S. Shioyama, in *Proceedings of the International Conference on Nuclear Structure, Tokyo, 1977*, edited by T. Marumori (Physical Society of Japan, Tokyo, 1978); J. Phys. Soc. Jpn. Suppl. 44, 298 (1978). In this reference, there was an error in the computer code that calculated the perturbation iteration. The correct value is given in Sec. IV of the present paper.

[20] Y. Yamaguchi and Y. Yamaguchi, Phys. Rev. 95, 1628, 1635 (1954).

[21] K. Meetz, J. Math. Phys. 3, 690 (1962); S. Weinberg, Phys. Rev. 130, 776 (1963); 131, 440 (1963).

[22] M. G. Fuda, Phys. Rev. 166, 1064 (1968).

[23] T. Sasakawa, Prog. Theor. Phys. Suppl. 27, 1 (1963).

[24] A. E. S. Green and T. Sawada, Rev. Mod. Phys. 39, 594 (1967); T. Ueda and A. E. S. Green, Phys. Rev. 174, 1304 (1968).

[25] T. Sasakawa and T. Sawada, Phys. Rev. C 11, 87 (1975).

[26] T. Janssens, R. Hofstadter, E. B. Hughes, and M. R. Yearian, Phys. Rev. 142, 922 (1966).

[27] J. S. McCarthy, I. Sick, and R. R. Whitney, Phys. Rev. C 15, 1396 (1977).

[28] H. Collard, R. Hofstadter, E. B. Hughes, A. Johansson, M. R. Yearian, R. B. Day, and R. T. Wagner, Phys. Rev. 138, B57 (1965).